

06.3

Magnetic selection of iron-based nanoparticles in pulsed laser synthesis

© D.A. Kochuev¹, A.S. Chernikov¹, U.E. Kurilova^{1–3}, A.A. Voznesenskaya¹,
A.F. Galkin¹, D.V. Abramov¹, A.V. Kazak^{1,4}, A.Yu. Gerasimenko^{2,3}, K.S. Khorkov¹

¹ Vladimir State University, Vladimir, Russia

² National Research University of Electronic Technology, Zelenograd, Moscow, Russia

³ I.M. Sechenov First Moscow State Medical University, Moscow, Russia

⁴ Moscow Polytechnic University, Moscow, Russia

E-mail: khorkov@vlsu.ru

Received December 29, 2023

Revised February 29, 2024

Accepted March 11, 2024

The paper presents the results of the ablative synthesis of iron nanoparticles in an argon medium under the action of nanosecond laser pulses. Nanoparticles were collected and deposited using a magnetic field. The effectiveness of the methods used for collecting iron-based nanoparticles is considered. The results of scanning electron microscopy of the obtained nanoparticles are presented.

Keywords: laser ablation, synthesis of iron nanoparticles, deposition of nanoparticles in a magnetic field.

DOI: 10.61011/TPL.2024.06.58484.19858

Although laser ablation is a fairly complex and multifactorial process, it opens up new opportunities for fabrication of various types of nanomaterials. The flexibility of control over physical processes in laser treatment and the potential to use additional sources of external effects for adjustment of the synthesis process are among the advantages of this approach. Metallic materials differ from non-metallic ones in that the laser radiation energy is absorbed by free electrons in them. Therefore, the lack of spectral selectivity ensures universal applicability of laser ablation in fabrication of nanostructures from all kinds of metals. The general principle of laser synthesis of nanomaterials forms the basis for various technologies involving the processing of targets in vacuum, gas, or liquids and the application of supplementary external fields [1–8]. The shape of the initial material also affects the end result. The rate of nanostructuring may be increased in laser processing of a laminar powder flow [9]. In the case of laser ablation in liquids, the confinement effect, which is manifested when ablated particles interact with each other in a cavitation bubble near the target surface in the course of nucleation and growth of nanostructures prior to dispersion in a liquid, exerts an additional influence [10,11]. Studies into nanoparticle (NP) production by laser ablation in electrostatic and magnetic fields revealed a reduction in both the average value and the spread of dimensions of formed structures [12,13]. The application of an external magnetic field provided an opportunity to produce NP chains by laser ablation in a liquid [14]. In the present study, the possibility of formation of such structures in a gas processing medium is demonstrated.

The wide variety of chemical and physical properties of iron and iron oxide NPs has motivated a great amount of recent research into these particles in biology and materials science. They have numerous potential applications,

including those in magnetic liquids, magnetic microdevices, magnetic hyperthermia, water purification, and guided drug delivery [15,16].

Magnetic iron oxide (FeO) nanoparticles encapsulated with biopolymers are used widely for local drug delivery guided by an external magnetic field, which helps minimize side effects, in cancer therapy. In practice, the optimum functional performance of FeO NPs is achieved when they have high magnetization values, a narrow size distribution, and specially encapsulated surfaces. Owing to their specific primary structure, nontoxicity, biocompatibility, and biodegradability biopolymers used for surface functionalization offer a number of advantages in biomedical applications. Functionalized FeO NPs offer various opportunities, including ligand, protein, and antibody targeting and covalent attachment of drugs for cancer treatment with the use of an external magnetic field [17–19]. Different methods for synthesis and surface modification of compound NPs of iron oxide and alloys and NPs of core/shell, dumbbell, and multicomponent types are being developed with the aim of making these particles biocompatible for multimodality imaging and targeted drug/gene delivery applications [20].

The diagram of the setup for ablation synthesis in a magnetic field is shown in Fig. 1. Ablation processing was performed using laser source 1 with a pulse duration of 100 ns, a pulse energy up to 1 mJ, and a wavelength of 1064 nm. The laser spot diameter on the target surface was 50 μm. A disk-shaped iron (99.95%) sample with a diameter of 10 mm and a thickness of 3 mm (2 in Fig. 1) was positioned on a heat-conducting plunger (holder 3) that was held steady in contact with retaining cylinder 4 and removed heat from the sample being processed. A gas mixture was pumped through the sample holder for cooling and removal of ablation products. The inlet channel was sealed with ring 5, which allowed for rapid sample

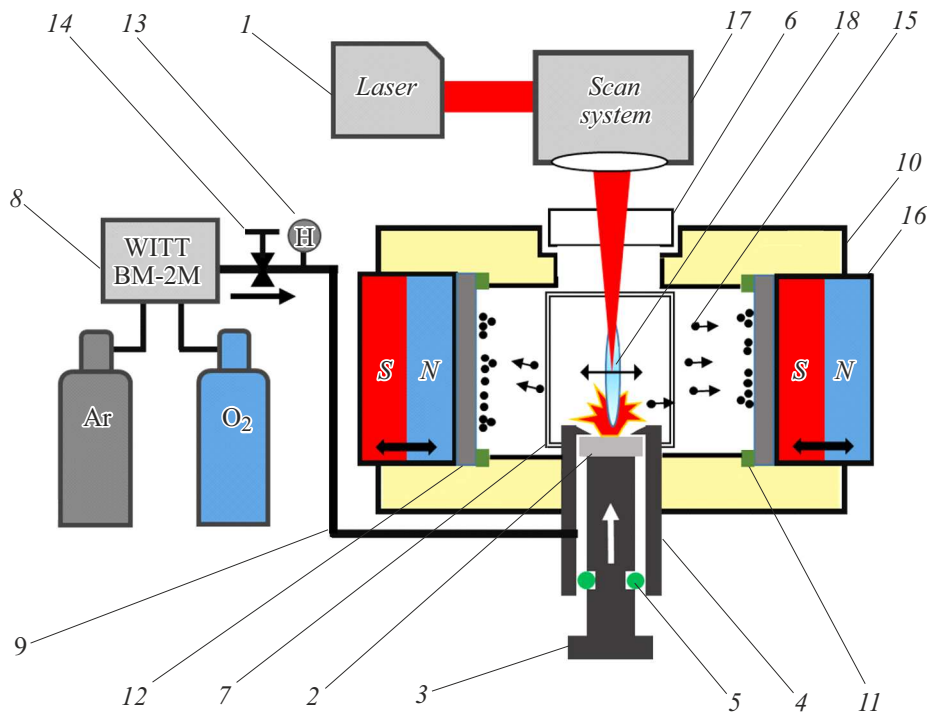


Figure 1. Diagram of the experimental setup for nanoparticle synthesis in a magnetic field.

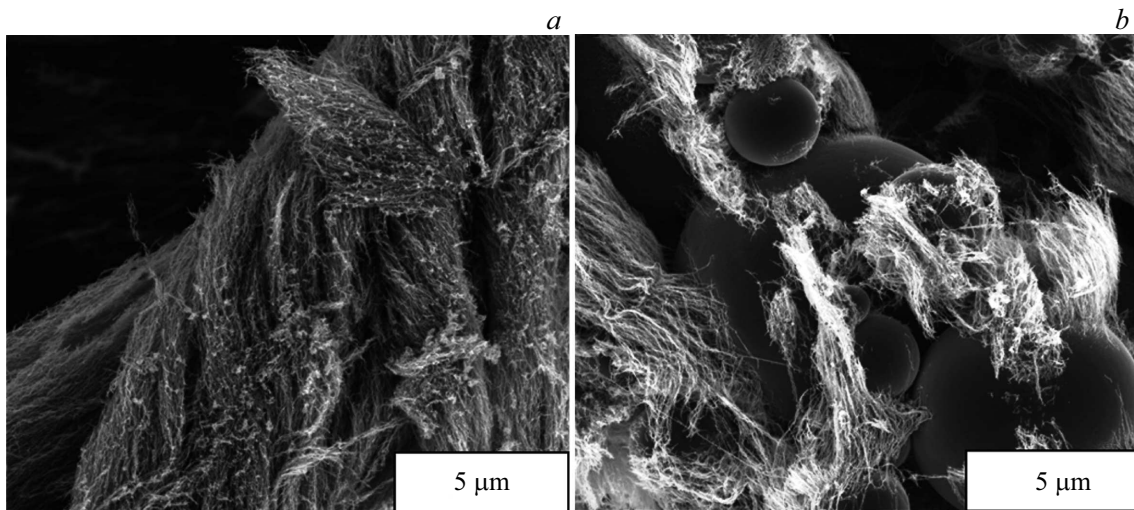


Figure 2. SEM images of nanoparticles produced in the process of laser ablation of iron in a magnetic field. *a* — The oxygen concentration is 30%, and the argon concentration is 70%; *b* — the oxygen concentration is 90%, and the argon concentration is 10%.

replacement by moving the plunger. Laser radiation was introduced through window 6. The alignment of the treated sample surface and the process of laser ablation in a magnetic field were monitored with a CCD camera through inspection window 7. The gas mixture flow through the chamber was regulated by turning the proportional mixing valve of gas mixer 8. The working chamber volume was filled with gas (argon/oxygen/proportional gas mixture) flowing from cylinders along line 9.

Pure iron nanoparticles were synthesized in argon. The average size of these nanoparticles is 15 nm. Iron oxide

nanoparticles with 95% of the magnetite phase may be formed if oxygen is added to the gas mixture. A further increase in oxygen concentration in the mixture leads to more intense heating of the processed sample region, raising the fractional concentration of particles larger than $10\ \mu\text{m}$. Prior to experiments, the chosen composition was blown through insulated vessel 10 at a flow rate of 11 l/min for 5 min. The gas mixture escaped from the chamber volume via service channels positioned in the region of the laser radiation input window. This approach provides an oppor-

tunity to perform selection of synthesized nanoparticles on the basis of magnetic moment.

In experiments, magnets were mounted with either like poles or unlike poles facing each other. No effect of the orientation of magnet poles on the properties of formed nanoparticles and the dynamics of laser ablation synthesis was found. The distance between magnets was set to 50 mm with the use of 5-mm-thick rings *11*. The rate of ablation synthesis of nanoparticles in these conditions was on the order of 250 mg/h. Nanoparticles deposited onto the surface of quartz plates were collected into containers for further analysis. Ablated particles were carried out of the chamber by gas-dynamic flows in the process of synthesis. In the case of oxygen deficiency in ablation in argon, particles carried out of the chamber are burnt down as a result of violent oxidation in contact with the environment (outside of the vessel). Synthesized particles expelled from the region of laser irradiation acquire magnetic properties only after cooling to a temperature below the Curie point (around 770°C).

Repeat irradiation of ablated particles is possible in laser ablation synthesis. This effect is suppressed by increasing the rate of gas mixture flow through the ablation processing zone. Particles with a nonzero magnetic moment leave the region of laser radiation propagation and are deposited onto the surface of quartz substrates *12* under the influence of magnetic fields. The pressure was monitored with gage *13* and adjusted by valve *14* to maintain a positive pressure of 0.1–2 bar within the working chamber. Ablated Fe and Fe₃O₄ particles (*15* in Fig. 1) were deposited under the influence of a magnetic field produced by permanent magnets *16*. The magnetic field strength on the surface was as high as 5000 G. A system of galvanometric scanners *17* was used for material processing. The use of magnets allowed us to remove particles from processing region *18*. The images obtained with a scanning electron microscope (SEM; see Fig. 2) revealed that nanoparticles deposited onto the surface of quartz glass substrates formed filamentary structures of a characteristic shape. Such structures were observed both for nanoparticles of pure iron (Fig. 2, *a*) and for nanoparticles in the magnetite phase (Fig. 2, *b*). Particles forming these filamentary structures are weakly agglomerated; in zero external magnetic field, they efficiently form colloidal systems in liquid media under the influence of ultrasonic vibrations. The phase composition of synthesized particles was determined using a D8 ADVANCE (Bruker) X-ray diffractometer.

It was established experimentally that iron-based nanoparticles with a nonzero magnetic moment may be produced both in an argon medium (pure iron) and in a mixture with an oxygen concentration upward of 35% (in the magnetite phase). The collection of iron-based nanoparticles is feasible only in a magnetic field, while magnetite based nanoparticles may be collected under the influence of electrostatic and magnetic fields.

Funding

The study into the processes of formation of nanoparticles was supported by the Russian Science Foundation (grant No. 22-79-10348). The preparation and analysis of samples were carried as part of the state assignment of the Ministry of Science and Higher Education of the Russian Federation, project FZUN-2020-0013.

Conflict of interest

The authors declare that they have no conflict of interest.

References

- [1] A.A. Ionin, S.I. Kudryashov, A.A. Samokhin, *Phys. Usp.*, **60** (2), 149 (2017). DOI: 10.3367/UFNe.2016.09.037974.
- [2] M.V. Shugaev, C. Wu, O. Armbruster, A. Naghilou, N. Brouwer, D.S. Ivanov, T.J.-Y. Derrien, N.M. Bulgakova, W. Kautek, B. Rethfeld, L.V. Zhigilei, *MRS Bull.*, **41** (12), 960 (2016). DOI: 10.1557/mrs.2016.274
- [3] N.A. Inogamov, Y.V. Petrov, V.A. Khokhlov, V.V. Zhakhovskii, *High Temp.*, **58** (4), 632 (2020). DOI: 10.1134/S0018151X20040045.
- [4] X. Wang, H. Yu, P. Li, Y. Zhang, Y. Wen, Y. Qiu, Z. Liu, Y. Li, L. Liu, *Opt. Laser Technol.*, **135**, 106687 (2021). DOI: 10.1016/j.optlastec.2020.106687
- [5] B. Guo, J. Sun, Y. Hua, N. Zhan, J. Jia, K. Chu, *Nanomanuf. Metrol.*, **3** (1), 26 (2020). DOI: 10.1007/s41871-020-00056-5
- [6] A.S. Chernikov, G.I. Tselikov, M.Yu. Gubin, A.V. Shesterikov, K.S. Khorkov, A.V. Syuy, G.A. Ermolaev, I.S. Kazantsev, R.I. Romanov, A.M. Markeev, A.A. Popov, G.V. Tikhonowski, O.O. Kapitanova, D.A. Kochuev, A.Yu. Leksin, D.I. Tselikov, A.V. Arsenin, A.V. Kabashin, V.S. Volkov, A.V. Prokhorov, *J. Mater. Chem. C*, **11** (10), 3493 (2023). DOI: 10.1039/D2TC05235K
- [7] K.S. Khorkov, D.A. Kochuev, V.A. Ilin, R.V. Chkalov, V.G. Prokoshev, *J. Phys.: Conf. Ser.*, **1400** (5), 055027 (2019). DOI: 10.1088/1742-6596/1400/5/055027
- [8] A.S. Chernikov, D.A. Kochuev, A.A. Voznesenskaya, A.V. Egorova, K.S. Khorkov, *J. Phys.: Conf. Ser.*, **2077** (1), 012002 (2021). DOI: 10.1088/1742-6596/2077/1/012002
- [9] M.F. Becker, J.W. Keto, D. Kovar, *Method for producing nanoparticles and nanostructured films*, patent US0287308A1 (Washington, DC, 2005).
- [10] S. Reich, P. Schönfeld, P. Wagener, A. Letzel, S. Ibrahimkuty, B. Gökce, S. Barcikowski, A. Menzel, T. dos Santos Rolo, A. Plech, *J. Coll. Interface Sci.*, **489**, 106 (2016). DOI: 10.1016/j.jcis.2016.08.030
- [11] A. Letzel, M. Santoro, J. Frohleiks, A.R. Ziefuß, S. Reich, A. Plech, E. Fazio, F. Neri, S. Barcikowski, B. Gökce, *Appl. Surf. Sci.*, **473**, 828 (2019). DOI: 10.1016/j.apsusc.2018.12.025
- [12] M. Razaghianpour, M. Hantehzadeh, A.H. Sari, E. Darabi, *Opt. Quantum Electron.*, **54** (10), 610 (2022). DOI: 10.1007/s11082-022-03964-6
- [13] M. Razaghianpour, M. Hantehzadeh, E. Darabi, *Microscopy Res. Tech.*, **84** (12), 3171 (2021). DOI: 10.1002/jemt.23875
- [14] J. Xiao, P. Liu, C.X. Wang, G.W. Yang, *Prog. Mater. Sci.*, **87**, 140 (2017). DOI: 10.1016/j.pmatsci.2017.02.004

- [15] A. Ali, H. Zafar, M. Zia, I. Ul Haq, A.R. Phull, J.S. Ali, A. Hussain, *Nanotechnol. Sci. Appl.*, **19** (9), 49 (2016). DOI: 10.2147/NSA.S99986
- [16] W. Ling, M. Wang, C. Xiong, D. Xie, Q. Chen, X. Chu, X. Qiu, Y. Li, X. Xiao, *J. Mater. Res.*, **34** (11), 1828 (2019). DOI: 10.1557/jmr.2019.129
- [17] D. Zhang, W. Choi, Y. Oshima, U. Wiedwald, S.H. Cho, H.P. Lin, Y. Ito, K. Sugioka, *Nanomaterials*, **8** (8), 631 (2018). DOI: 10.3390/nano8080631
- [18] S.O. Aisida, P.A. Akpa, I. Ahmad, T-K. Zhao, M. Maaza, F.I. Ezema, *Eur. Polym. J.*, **122**, 109371 (2020). DOI: 10.1016/j.eurpolymj.2019.109371
- [19] U.E. Kurilova, A.S. Chernikov, D.A. Kochuev, L.S. Volkova, A.A. Voznesenskaya, R.V. Chkalov, D.V. Abramov, A.V. Kazak, I.A. Suetina, M.V. Mezentseva, L.I. Russu, A.Yu. Gerasimenko, K.S. Khorkov, *J. Biomed. Photon. Eng.*, **9** (2), 020301 (2023). DOI: 10.18287/JPPE23.09.020301
- [20] R. Hao, R. Xing, Z. Xu, Y. Hou, S. Gao, S. Sun, *Adv. Mater.*, **22** (25), 2729 (2010). DOI: 10.1002/adma.201000260

Translated by D.Safin